

Surface motion of active rock glaciers in the Sierra Nevada, California, USA: inventory and a case study using InSAR

Lin Liu¹, C. I. Millar², R. D. Westfall², and H. A. Zebker¹

¹Department of Geophysics, Stanford University, Stanford, CA, USA

²USDA Forest Service, Pacific Southwest Research Station, Albany, CA, USA

Correspondence to: Lin Liu (liulin@stanford.edu)

Abstract. Despite the abundance of rock glaciers in the Sierra Nevada of California, USA, few efforts have been made to measure their surface flow. Here we use the interferometric synthetic aperture radar (InSAR) technique to compile a benchmark inventory describing the kinematic state of 59 active rock glaciers in this region. In the late summer of 2007, these rock glaciers moved at speeds **that** range from 14 cm_{yr}⁻¹ to 87 cm_{yr}⁻¹ with a mean value of 53 cm_{yr}⁻¹. Our inventory reveals a spatial difference: rock glaciers in the southern Sierra Nevada moved faster than the ones in the central Sierra Nevada. In addition to the regional mapping, we also conduct a case study to measure the surface flow of the Mount Gibbs rock glacier in fine spatial and temporal detail. The InSAR measurements over this target reveal (1) that the spatial pattern of flow is **correlated** **with** surface geomorphic features and (2) a significant seasonal variation of flow speed whose peak value was 48 cm_{yr}⁻¹ in the fall **of 2007**, more than twice the minimum value observed in the spring **of 2008**. The seasonal variation lagged air temperatures by three months and likely results from temporal changes in mechanical strength of mixing debris and ice, internal melting of ice, and surface snow cover. Our finding on the seasonal variation of surface speed reinforces the importance of a long time series with high temporal sampling rates to detect possible long-term changes of rock glacier **kinematics** in a warming climate.

1 Introduction

Rock glaciers are tongue- or lobate-shaped landforms on high mountain slopes, typically consisting of mixtures of unconsolidated rock debris and ice. Rock glaciers are of geomorphic, climatic, and hydrological importance in alpine periglacial environments. They are visible indicators of permafrost

and contribute to a major portion of mass transport of the alpine landforms (Barsch, 1977; Humlum, 2000; Brenning, 2005; Degenhardt, 2009). In addition, they preserve a long geological history in ice records and thus provide information and insights on paleoclimate (Clark et al., 1994; Humlum, 1998; Haeberli et al., 1999; Konrad et al., 1999; Harrison et al., 2008). Finally, they prolong ice melt and sustain surface runoff **in dry years**, acting as water reserves that are especially important in semi-arid mountain areas (Burger et al., 1999; Brenning, 2005; Croce and Milana, 2002; Millar et al., 2012).

Surface kinematics is a fundamental physical state of rock glaciers. Active rock glaciers creep downslope cohesively as a consequence of the deformation of internal ice. Surface flow is related to regional forcing including climatic conditions and local factors such as thickness, topographic relief, duration of solar radiation, lithology, and internal structures (Johnson et al., 2007; Käab et al., 2007). Therefore, temporal variation in surface kinematics sheds light into changes in regional and local conditions.

Possible change of rock glacier flow in response to ongoing climate warming is also an intriguing and important problem. Compared to ice glaciers, rock glaciers are believed to be less sensitive to rising temperature due to isolation of rock mantles (Clark et al., 1994; Barsch, 1996). However, there are also emerging observations suggesting that rock glaciers in the European Alps have increased flow rates since circa 1990 (e.g. Käab et al., 1997; Krainer and Mostler, 2000; Delaloye et al., 2008; Nötzli and Vonder Muehll, 2010).

Both field and remote sensing methods have been used to measure rock glacier surface flow. Repeat geodetic surveys map surface displacement at selected ground markers, usually a few years apart (e.g. Wahrhaftig and Cox, 1959; Barsch, 1996; Berger et al., 2004; Berthling et al., 1998; Konrad et al., 1999; Lambiel and Delaloye, 2004; Isaksen et al., 2000). **Some recent efforts installed permanent global positioning system receivers on rock glaciers for continuous monitoring** (e.g. Limpach et al., 2011). Due to the remote locations of rock glaciers in high mountains, field observations are usually scarce and do not provide a complete view of rock glacier movement and processes. Remote sensing techniques such as repeat photogrammetry (e.g. Käab et al., 1997; Käab, 2002) and terrestrial laser scanning (Avian et al., 2009) have proved to be especially useful to fill the spatial gaps.

In contrast to optical sensors, microwave interferometric synthetic aperture radar (InSAR) measures ground deformation day-or-night in all weather conditions. The spatial extent of many space-borne SAR images is approximately 100 km wide and several hundreds of km long. Most InSAR deformation maps have a spatial resolution as fine as 10 m. These merits make InSAR a unique tool for measuring rock glaciers flow kinematics including (1) inventory mapping and (2) detailed case studies on individual rock glaciers. The latter capability has been demonstrated at targets around the world (Rott and Siegel, 1999; Nagler et al., 2002; Rignot et al., 2002; Kenyi and Kaufmann, 2003; Strozzi et al., 2004). **Additionally, active rock glaciers have sparse vegetation cover, making**

them good InSAR targets as the temporal decorrelation problem due to vegetation changes is largely avoided (Zebker and Villasenor, 1992).

60 In this study we use the InSAR technique to map surface motion of rock glaciers in the Sierra Nevada of California, USA. Despite their abundance in this region, rock glaciers are largely overlooked. They have been recently brought to wider attention partly thanks to the inventory compiled by Millar and Westfall (2008) based on their field studies. This is hereafter referred to as the “MW database”, which is available at the National Snow and Ice Data Center
65 <http://nsidc.org/data/ggd652.html>. Still, little is known about their kinematic states, let alone the long-term changes in surface flow.

Our first objective is to conduct a quantitative and nearly spatially-complete assessment on the kinematic behaviors of the active rock glaciers in the Sierra Nevada. Using space-borne InSAR data, we compile a georeferenced inventory to describe flow speed, aspect direction, mean slope and area
70 of active motion of active rock glaciers in the region. To our knowledge, this is the first InSAR study on rock glaciers in the Sierra Nevada. Our regional-scale mapping effort on rock glaciers is the only one outside the Swiss Alps (Delaloye et al., 2010). Regional survey is difficult to accomplish logistically by field measurements. As a secondary product of the InSAR study, we are also able to identify rock glaciers based on their distinct kinematic behaviors from stable surroundings. Some
75 of these rock glaciers have been overlooked in field studies due to their remoteness and their similar appearance to moraines and scree slopes (Millar and Westfall, 2008). For the latter reason, it is also difficult to spot a few rock glaciers on optical remote sensing images.

Our second objective is to focus on a single target, the Mount Gibbs rock glacier, to image its surface motion at a fine spatial resolution and investigate its seasonal variation. Previous remote-
80 sensing studies, including InSAR, only provided a single snapshot of surface motion over periods ranging from one day to a few years. Our case study on the Mount Gibbs rock glacier for the first time detects a significant seasonal variability of surface motion from space.

2 Rock glaciers in the Sierra Nevada of California

2.1 Overview

85 The Sierra Nevada is a major mountain range located between the Central Valley and the Basin and Range province in California. It has warm Mediterranean and semi-arid climates, characterized by warm dry summers and cool wet winters. **Snow precipitation occurs between November and May, with a modest late winter peak** (Serreze et al., 1999). The entire region was heavily glaciated during the Pleistocene (Clark and Gillespie, 1997). A few small ice glaciers and persistent snow fields are
90 scattered at cirques in the high mountains. The glaciers are of Late Holocene origin and not relicts from the Pleistocene. Decomposed rock is abundant, especially along metamorphic exposures of the eastern escarpment.

Rock glaciers and related landforms are common throughout cirques and valleys of the central and southern parts of the range. Our study area extends from north of Bridgeport to Lone Pine as shown in Fig. 1. Millar and Westfall (2008) mapped more than 280 rock glaciers in this area. Most of these rock glaciers are clearly visible in remote sensing optical imagery such as Google Earth images and air photos (more in Sect. 4.1 and Fig. 3). According to their different locations, origins, and shapes, Millar and Westfall (2008) further grouped the rock glaciers into two classes: cirque rock glaciers and valley wall rock glaciers. Cirque rock glaciers originate in high cirques and flow parallel to the valley axis as long-lobed debris bodies. They often have an ice or snow field at the cirque wall and arcuate flow lines on the debris surface. The MW database lists 184 cirque rock glaciers, 67 % of which are active and have a mean elevation of 3390 m and a mean size of 20 ha. Valley wall rock glaciers, instead, occur on valley walls and are characterized by wide wedge-shaped structures. The MW database includes 105 valley rock glaciers, 61 % of which are active and have a mean elevation of 3292 m and a mean size of 3 ha, much smaller than the cirque rock glaciers.

2.2 Mount Gibbs rock glacier

The Mount Gibbs rock glacier is centered at $37^{\circ}53'44''$ N, $119^{\circ}12'13''$ W and is located in Gibbs Canyon along the eastern escarpment of the Sierra Nevada. Its ground and aerial photos are shown in Figs. 2 and 5a, respectively. This tongue-shaped rock glacier is approximately 700 m long in its flow direction and 300 m wide. Its geometry suggests that the rock glacier flows downslope initially in a N-NE direction and then bends toward the NE and E-NE. Its head is a bowl-shaped cirque wall surrounded by Mount Gibbs (3893 m a.s.l.) and Mount Dana (3980 m a.s.l.). A small ice glacier is perched in the adjacent and hanging cirque to the east of the rock glacier. Complex meta-volcanic and meta-sedimentary rocks form mountains of this region (Kistler, 1966). The rock glacier surface is covered by angular and poorly-sorted graywackes that are gray-colored meta-sedimentary rocks. Transverse furrows and longitudinal ridges are visible along two lobes in the middle and lower parts. The terminus of the rock glacier is an over-steepened face and forms the southwest shore of Kidney Lake. To the east of the rock glacier terminus is glacial till that extends into the lake and forms the lake's concave shoreline. The glacial till (labeled in Fig. 2) is not part of the rock glacier but originates from the ice glacier at the peak of Mount Gibbs.

We choose the Mount Gibbs rock glacier for a detailed kinematic study because of several reasons. Although it is similar to other active cirque rock glacier in the MW database in elevation and size, the Mount Gibbs rock glacier has a complex geometry and thus an interesting target for mapping surface flow at fine spatial resolution. From the perspective of InSAR processing (see more in Sect. 3.2), this rock glacier is ideal because of its NE flow direction, moderate flow speed, and large debris-covered area. Practically, radar images from two satellite tracks were acquired continuously over this rock glacier (see Sect. 3.1), making it possible to conduct a detailed time series study.

3 Methods

In this section, we first present technical details of InSAR processing for the case study on the Mount Gibbs rock glacier (Sect. 3.1). Then we describe a similar but simplified strategy for the regional survey and also list criteria for including an active rock glacier in our inventory (Sect. 3.2).

3.1 InSAR data and processing for case study

For the case study on the Mount Gibbs rock glacier, we apply InSAR processing using a motion-compensation strategy (Zebker et al., 2010) to the Phased Array type L-band Synthetic Aperture Radar (PALSAR) data acquired by the Japanese Advanced Land Observing Satellite (ALOS). By measuring phase differences between two radar images taken at different times, InSAR constructs an interferogram that maps ground surface displacement along the line-of-sight (LOS) direction during the time interval of the two images. To maximize the temporal sampling rates of ground deformation from spring 2007 to spring 2008, we use the PALSAR data acquired along two ascending paths: Path 216/Frame 750 and Path 217/Frame 740. Unfortunately, no descending path PALSAR scenes were acquired by the ALOS satellite over this area. **Scenes acquired in other years are not available to us either.** We take spatial average of every two pixels in the azimuth direction on each interferogram to achieve a ground resolution of approximately 10 m by 10 m. Accordingly, we use a 1/3 arc-second (approximately 10 m) digital elevation model (DEM) from the USGS National Elevation Database to remove the topographic contribution. **The DEM was produced using data acquired during 1999 and 2001 and has a quoted vertical accuracy of 3 m (Gesch et al., 2002). The possible elevation changes between DEM date and PALSAR acquisitions could cause InSAR deformation errors that are linearly correlated with the perpendicular baseline. Such topographic errors are estimated and removed in time series analysis (see below).**

We produce a total of 12 interferograms and list them in Table 1. All interferograms have a short time span as we want to minimize InSAR phase decorrelation due to fast ground motion and to better detect seasonal variability of ground motion. The repeat orbit cycle of the ALOS satellite limits the shortest time span to 46 days. We use the SNAPHU software (Chen and Zebker, 2002) for phase unwrapping, i.e. the process to reconstruct the absolute phase from the InSAR observable: the 2π modulus of the absolute phase. We also choose a reference point ($37^{\circ}54'0''$ N, $119^{\circ}11'44''$ W) outside the rock glacier where we assume zero displacement.

To determine the ground surface motion, we project the InSAR-measured LOS displacements onto the downslope direction, assuming that surface-parallel flow follows the steepest slope direction on the rock glacier surface. The InSAR LOS vector is determined by two angles: the heading angle of satellite flight path, denoted as α , and the incidence angle θ_{inc} (i.e. the angle between the incident radar waves and the direction normal to the ground surface). Along both paths, the heading angles are the same: 13.5° counter-clockwise from north. Within the rock glacier area, the incidence angles

are 37.5° and 40.3° for Paths 216 and 217, respectively. We use the DEM to calculate local slope angle θ_{slp} and azimuth angle β and then use the following mapping function to convert the LOS displacement (D_{LOS}) to the downslope displacement (D):

$$D = \frac{D_{\text{LOS}}}{\sin(\alpha - \beta) \sin \theta_{\text{inc}} \cos \theta_{\text{slp}} + \cos \theta_{\text{inc}} \sin \theta_{\text{slp}}}. \quad (1)$$

For each interferogram, we divide the InSAR-estimated downslope displacement by the time interval and obtain the annual equivalent speed.

We also calculate time series of surface speed at selected high coherence points. From each set of geocoded interferograms grouped according to their paths, we use the small baseline subset inversion method (Berardino et al., 2002) to estimate surface speed during two consecutive acquisition times as well as topographic errors. We then combine these two sets of speed estimates to obtain a continuous time series from spring 2007 to spring 2008. We assume that the tropospheric artifacts are uniform within this small area so that we do not apply any atmospheric filtering in the time series inversion.

3.2 Inventory mapping using InSAR

For regional mapping, we identify the rock glaciers by manually inspecting moving features on interferograms. Instead of time series analysis using multiple interferograms, we only construct one interferogram from each ALOS PALSAR frame (roughly 100 km by 70 km). Our study area (Fig. 1) is approximately 240 km by 150 km and is completely covered by five frames: Frames 720, 730, and 740 in Path 216 and Frames 740 and 750 in Path 217. For each frame in Path 216, we construct one interferogram by applying the same InSAR processing methods described in Sect. 3.1 to the PALSAR data acquired on 18 August 2007 and 3 October 2007. Similarly for Path 217, we construct one interferogram for each frame using the data acquired on 4 September 2007 and 20 October 2007. Figure 3a shows a portion of the Path 216/Frame 730 interferogram as an example that reveals moving rock glaciers standing out from surrounding landforms. For comparison, we also show optical images taken in the summer of 1999 in Fig. 3b–d, in which rock glaciers appear similar to their surroundings.

Constrained by the capability of InSAR for mapping small targets in mountain areas, there are a few limitations on the size, flow speed, and location of a rock glacier to be included in our inventory. First, InSAR can only measure surface flow over the debris-covered area where the interferometric coherence is sufficiently high. Decorrelation in interferometry phase is common at the head due to fast motion of glacier ice. Second, the debris-covered area of a rock glacier must be larger than 2 ha to be reliably identified. For instance, the Fig. 3a interferogram barely resolves surface motion over the small rock glacier outlined by the red box in Fig. 3c. Third, at each rock glacier, the displacement component of the total phase must be significantly larger than decorrelation noise, here assumed 1 cm. For a 46-day-span interferogram, this lower bound on the flow speed is equivalent to 10 cm yr^{-1} . Fourth, we are unable to map any rock glaciers located within the radar shadow

or layover zones that facing the radar illumination. In the viewing geometry of ascending frames
200 used in this study, layover zones are on the western slopes and appear as bright stripes (outlined in
Fig. 3a). Lastly, also limited by the viewing geometry, we are unable to identify any rock glaciers
moving parallel to the satellite flight direction using the conventional cross-track InSAR technique.
This is likely the reason that the rock glacier outlined by the red box in Fig. 3d appears not moving
in the interferogram and thus is excluded in our inventory.

205 We also use additional data including the MW database and Google Earth images as aids to iden-
tifying rock glaciers from interferograms. Interferograms simply measure surface motion; and they
alone cannot tell the origin of surface motion. In addition to rock glaciers, surface motion may occur
at several other types of geomorphic features in the Sierra Nevada, including soil solifluction by
mass wasting, boulder streams, debris flows, landslide slumping, avalanches, rock fall/slides, and
210 regular ice glaciers. Of these features, soil solifluction and boulder streams are akin to rock glaciers,
and their motion can be generalized as periglacial surface creep. Locations for soil solifluction and
boulder streams are listed in the MW database, which is used to these features from our rock glacier
inventory. All other features typically move at speeds at least one order of magnitude higher than
rock glaciers, and therefore lose coherence in our 46-day-long ALOS interferograms. These fea-
215 tures also have distinct geomorphic characteristics and can be easily separated from rock glaciers by
visually inspecting Google Earth images.

For each identified active rock glacier, our inventory lists the size, flow speed and aspect direction
based on the InSAR measurements, the mean slope and elevation based on the DEM. Similar to
the Mount Gibbs rock glacier study, we choose a local reference point near but outside each rock
220 glacier to calibrate the flow speed measurements. Using the geocoded interferograms, we measure
the dimensions along and across flow direction of each active rock glacier, whose area is not always
the same as the area of apparently active moraines shown on optical images. Similar to the Mount
Gibbs rock glacier study, we use site-wise incidence angles and mean local surface slopes to convert
the InSAR LOS displacement into downslope motion using Eq. (1) for all rock glaciers. We use the
225 equivalent annual speed at the center of each rock glacier to represent its kinematic state.

4 Results

4.1 Regional inventory

Our database describes the kinematic states of 59 active rock glaciers in central and southern Sierra
Nevada. Their size and surface flow speed in the late summer of 2007 are plotted in Fig. 1. We pro-
230 vide the complete inventory in the Supplement, including a Google Earth KMZ file and a spreadsheet
that provides all quantitative information. Table 2 summarizes the mean values of major parameters.
The mean flow speed was 55 cm yr^{-1} , with the fastest one moving at 84 cm yr^{-1} and the slowest
one moving at 15 cm yr^{-1} . They have a mean elevation of 3551 m and a mean size of 13 ha.

Our complete regional survey reveals several important spatial patterns of rock glacier kinematics
235 in the Sierra Nevada. The histogram of the azimuthal distribution (Fig. 4) indicates a pronounced
dominance of rock glaciers facing the N-NE direction. This is common for rock glaciers and normal
ice glaciers to form in the northern hemisphere because of the solar radiation aspect. Snow accumu-
lation due to drifts from SW winds and snow avalanching in this region may also contribute to such
N-NE dominance.

240 Regional map (Fig. 1) shows that active rock glaciers tend to cluster to each other, implying
a significant influence of regional conditions such as climate and topography on their occurrence.
There is a spatial gap in the mountain areas near Mammoth Lake where elevation is lower than
3000 m. Rock glaciers in the southern Sierra Nevada moved at a mean speed of 56 cm yr^{-1} , faster
than the ones in the central Sierra Nevada whose mean speed was 39 cm yr^{-1} . Considering the stan-
245 dard deviation values of these two sub-regional groups: 15 cm yr^{-1} for the southern area and 8 cm
 yr^{-1} for the central area, we conclude that the spatial difference in mean speeds is significant. We
speculate that such a regional difference, which is also visually evident in Fig. 1, is related to the
topographic relief. Compared with the ones in the central Sierra Nevada, rock glaciers in the South-
ern Sierra Nevada occur on cirques with greater relief (steeper slopes and lower basins), resulting in
250 more rock sliding and less solar radiation (Johnson et al., 2007), both contributing to faster speeds.

Another spatial contrast is that rock glacier speeds were less uniform in the southern area than
in the central Sierra Nevada. Within some valleys in the southern area, such as the ones shown in
Fig. 3, we observe a significant spatial variation in kinematic behaviors. It suggests strong influences
of local factors such as thickness, ice content, hydrological conditions, and debris content on surface
255 speed. Quantitative investigation on the correlation between surface speed and these local factors
requires a multivariate statistical analysis, which is out of the scope of this study.

We compare our inventory with the MW database in terms of rock glacier classes and locations.
All of our identified active features fall into the cirque rock glacier class defined by Millar and
Westfall (2008). However, only 14 (or 24 %) of them are collocated with the “active” ones in the
260 MW database. Millar and Westfall (2008) used the term “active” based on the geomorphic and
hydrological features, which may not all be actively moving. Our mapping method using InSAR is
a direct measurement of surface flow motion and thus ensures that the identified targets are moving
at a minimum speed of 10 cm yr^{-1} . In addition, 16 “active” cirque rock glaciers in the MW database
are not included in our inventory because they are smaller than 2 ha. We exclude 12 of MW’s
265 “active” rock glaciers, for instance, 7 in the Piute Pass Glacier divide (37.23° N , 118.75° W), because
they are either in the radar shadow zones or almost completely covered by ice. However, on the
positive side, our inventory includes 44 active rock glaciers that not identified in the MW database
from field work. For instance, within the region of Fig. 3, the MW database only includes one rock
glacier (i.e. the South Fork rock glacier as shown in Fig. 3b). Overall, we conclude that our inventory
270 based on InSAR and the MW database are complementary to each other; and together they provide

a more complete and valuable dataset.

4.2 Surface flow of the Mount Gibbs rock glacier

In this subsection, we present the InSAR results on the surface flow at the Mount Gibbs rock glacier. We first show the spatial variability that is correlated with surface geomorphic features. We then provide a time series of surface flow speed showing its seasonal variation during 2007–2008 and its delay behind air temperature. Such a seasonal variability has not been observed previously using remote sensing methods.

On individual targets, InSAR provides a more spatially complete assessment of the surface flow than field measurements. Fig. 5b shows the InSAR LOS speed over the Mount Gibbs rock glacier between 4 September 2007 and 5 December 2007. It clearly maps out two rapidly-flowing lobes (centered at “A” and “B”) at speeds of $\sim 50 \text{ cm yr}^{-1}$ and starting from the middle section of the rock glacier. Along both lobes, InSAR LOS speed decreases towards the rock glacier terminus. Such gradients in speed correlates well with surface ridges and furrows and suggest that these are geomorphic features caused by longitudinal compression. Fig. 5b also shows rapid surface motion ($> 60 \text{ cm yr}^{-1}$) near the head of the rock glacier (centered at “C”), although we cannot distinguish if this is motion of the normal glacier ice or rock debris beneath it. Additionally, this InSAR map reveals stable areas such as the southeast flank and the depression area between the two flowing branches. Other InSAR maps using different interferograms show a similar pattern but vary in magnitude.

Our time series analysis shows a strong seasonal variation of surface speed. In Fig. 6, each triangle represents the mean downslope speed at the marker “A” in Fig. 5b during the two consecutive PALSAR images in the same path, with the error bar showing the $1-\sigma$ uncertainty. The time series shows that the surface flow was slow in the spring, gradually increased throughout the summer, peaked in the fall at 48 cm yr^{-1} , and then abruptly slowed in the winter, reaching to the minimum of 22 cm yr^{-1} in the following spring. This seasonal variation had a phase lag behind the annual cycle of air temperature shown as the solid line in Fig. 6. Taking into account the uncertainties and the temporal intervals of speed estimates, we estimate that the phase delay value ranges from one to four months with a median of three months. We calculate the climatic air temperature at the rock glacier using the 1981–2010 mean air temperature records measured at Lee Vining (see its location in Fig. 1) and a temperature lapse rate of $-6.5 \text{ }^\circ\text{C km}^{-1}$ (Lundquist and Cayan, 2007; Millar and Westfall, 2008) to account for the elevation difference. This estimated temperature is consistent with the field measurements (Millar et al., 2012) and the Parameter-elevation Regressions on Independent Slopes Model (PRISM) outputs (Daly et al., 1994).

5 Discussion

305 5.1 Strengths and weaknesses of InSAR-based rock glacier inventory

We have demonstrated that InSAR provides quantitative information on the surface flow of rock glaciers in a spatial scale of a major mountain range. The InSAR survey is valuable: it reveals spatial patterns of rock glacier kinematics and provides benchmark information for studying the relationship between regional and local forcing conditions and rock glacier speed and for long-term
310 monitoring efforts. The InSAR survey is unique: it quantifies rock glacier speed, which is difficult to measure in the field. Inventory mapping using InSAR is also more complete than optical studies that are usually limited by cloud covers. In fact, InSAR and optical remote sensing techniques are complementary as the latter can provide 2-D velocities at even higher (e.g. sub-meter) spatial resolution (e.g. Roer et al., 2005) and it is not limited by the layover problem (see below).

315 However, our InSAR-based inventory is still incomplete. Explained in Sect. 3.2, our inventory only includes rock glaciers that are larger than 2 ha, moving faster than 10 cm yr^{-1} , located outside radar layover (western slopes) and shadow zones, and flowing non-parallel to the satellite flight direction. The lower bound on flow speed could be relaxed using interferograms spanning longer periods, provided that high coherence is maintained. The location constraints are not severe in the
320 Sierra Nevada because most active rock glaciers are located on the eastern (leeward) slopes, where snow precipitation is substantially less than the western slopes.

Our InSAR-based flow speed estimates are not free of errors. Deformation signals in one interferogram are contaminated by decorrelation noises, atmospheric artifacts, snow cover (more discussion below), and DEM errors. However, these errors are not correlated in time could be reduced using
325 multiple interferograms. We may also over-estimate the annual rock glacier speeds by using late-summer interferograms, as the case study on the Mount Gibbs rock glacier suggests that the annually-mean speed is likely smaller than the late-summer speed.

Temporal changes of snow cover and depth may cause (1) the InSAR decorrelation problem due to changes of surface dielectric properties and (2) InSAR phase errors due to refraction of radar waves
330 in snow (Guneriussen et al., 2001). Snow cover and depth in the California Sierra Nevada of California vary dramatically in time and in space (from mountain ranges to ranges); but no ground-based measurements is available at rock glaciers. Snow models such as the Snow Data Assimilation System (SNODAS, <http://www.nohrsc.nws.gov/nsa/>) could be used to estimate the snow water equivalent at any given location, which is the key parameter to estimate the phase shift due to snow cover
335 (Guneriussen et al., 2001). However, recent studies on improving the SNODAS model suggest that the model underestimates snow accumulation in lee sides of high cirques (Clow et al., 2012), exactly as in the Mount Gibbs high cirque. All these limitations make it a major challenge to accurately quantify the snow-related errors in our InSAR measurements.

Realistically, in the Mount Gibbs rock glacier case, we find that snow cover in winters has little

340 impact on our InSAR measurements, mainly for two reasons. First, the L-band radar waves can easily penetrate through dry snow in this area, and we observe little reduction in InSAR coherence in winter interferograms. Second, the snow distribution is almost constant within a relatively small area of a rock glacier and its adjacent surrounding, which results in a constant phase shift over the rock glacier and the reference point right outside the rock glacier. Since we calculate the surface motion
345 over the rock glacier by subtracting the phase at the reference point from the entire rock glacier, the error due to snow has largely been removed. Our inventory mapping uses satellite data acquired during snow-free seasons and is thus not subject to snow-related errors.

5.2 Causes of seasonal variation in flow speed at the Mount Gibbs rock glacier

According to the InSAR observations at the Mount Gibbs rock glacier (Fig. 6), seasonal variation
350 of surface flow speed is significant, more than double from the minimum in the spring to the maximum in the fall. Limited by data availability, we are only able to conduct such time series study for the 2007-2008 season. Nevertheless, our study adds one more finding to the few observations on seasonal variation of rock glacier speed (Haeberli, 1985; Arenson et al., 2002; Käab et al., 2007; Perruchoud and Delaloye, 2007; Ikeda et al., 2008). Both the magnitude and the temporal delay of
355 seasonal variability behind air temperature are comparable with the ground-based measurements at the Muragl (Arenson et al., 2002; Käab et al., 2007) and the Becs-de-Bosson rock glaciers (Perruchoud and Delaloye, 2007) in the Swiss Alps.

The exact cause(s) of the speed seasonal variations at the Mount Gibbs rock glacier is unclear. It might be partly due to the changes of rock glacier mechanical strength and rheology with ground
360 temperature. We model the thermal diffusion of ground warming and the increase of the creep parameter of rock glacier materials using the same method of Käab et al. (2007). We find that the modeled seasonal variation in surface speed is approximately 5 % of the annual mean value, much smaller than the InSAR-observed 50 % variations. Käab et al. (2007) found a similar discrepancy between the in-situ observations and the modeled speed variations that are solely driven by thermal diffusion. Even if we include a thin layer of highly deformable frozen material (Wagner, 1992; Arenson et al., 2002) in the flow model, the modeled seasonal variation is still less than 10 %.

Other possible mechanisms for seasonal variations include melting water penetration, basal sliding, and winter snow cover. Field investigations and water temperature measurements in the rock glacier talus outlet springs suggest persistent flow of water throughout the year (Millar et al., 2012).
370 The water sources include melting of surface snow and melting of internal ice due to thermal diffusion and warming effects of penetrated water. It takes time for internal ice to melt and for sufficient water to accumulate at the bottom of the rock glacier to act as a lubricant for basal sliding. Nonetheless, only a few studies have discussed the idea of basal sliding (Haeberli, 1985; Whalley and Martin, 1992) and it is unclear how commonly this mechanism occurs under rock glaciers. Ikeda et al. (2008)
375 proposed that snowmelt water could infiltrate into the frozen debris and modulate surface motion of

rock glaciers. However, their model predicts an increase in surface speed in early summer (May and June), different from our observations at the Mount Gibbs rock glacier. The delay of seasonal minimum speed that occurred in spring is likely caused by the refreezing of pore water and the winter snow cover, which insulates the ground from cold air and thus maintains surface speed. Modeling these mechanical and hydrological effects on rock glacier motion and its seasonal variation is a subject of future work.

5.3 Response of rock glaciers to climate warming: perspectives from InSAR

The kinematic response of rock glaciers to climate warming is contentious. The annual temperature in the Sierra Nevada is projected to rise by 2 to 4 °C by the end of the 21st century (Maurer, 2007). But it is unclear whether rock glaciers will speed up due to accelerated degradation and melting and higher erosion rates (Gruber and Haeberli, 2007) or remain stable due to (1) thermal insulation by the protective rock debris matrix (Clark et al., 1994; Barsch, 1996; Millar et al., 2012) and (2) the local cooling effects caused by air circulation within rock matrix (Juliussen and Humlum, 2008; Leopold et al., 2011). Flow speed of some rock glaciers in the European Alps have accelerated in the last two decades or so (e.g. Kääh et al., 1997; Krainer and Mostler, 2000; Delaloye et al., 2008; Bodin et al., 2009). By contrast, in the Rocky Mountains of the USA, even observations longer than 30 years show no significant changes in rock glacier speed (Potter et al., 1998; Janke, 2005).

Practically, the ALOS PALSAR data are too short for monitoring long-term changes in rock glacier flow as the satellite was in operation for only five years from late 2006 to early 2011. Nonetheless, our study strongly suggests the necessity of considering possible aliasing due to seasonal variation when estimating long-term changes in flow speed. Possible inter-annual variation in surface flow, which has been observed in the European Alps (Nöetzli and Vonder Muehll, 2010), further complicates the estimate of long-term trends. In general, it requires a long time series with high temporal sampling rates to separate possible long-term changes in rock glacier kinematics from seasonal and inter-annual variability. Other satellites such as ERS-1/2 and Envisat acquired longer time series of SAR data that are of potential for investigating response of rock glaciers in the Sierra Nevada to climate changes in the last two decades. The major challenge of using C-band data for rock glacier studies, however, is the problem of InSAR phase decorrelation due to fast surface flow. We suggest a strategy to form a long time series of interferograms that have short time spans (e.g. 35 days for ERS-1/2). The ERS-1/2 tandem (1-day intervals) and ice-phase (3-day intervals) data that are commonly used for ice glacier studies may not be useful because rock glacier motion within one day is of the order of 1 mm, too small to be reliably detected by InSAR. A few recently launched and future InSAR missions such as the TerraSAR-X, the Cosmo-SkyMed, and the Sentinel Satellites will continue the observation period and provide denser temporal sampling rates (e.g. 11 days of TerraSAR-X) for monitoring rock glaciers.

6 Conclusions

In summary, we use InSAR data to compile an inventory of the flow speed, direction, and area of active motion at 59 rock glaciers in the Sierra Nevada. In the late summer of 2007, these rock glaciers moved at a mean speed of 55 cm yr^{-1} . Spatially, rock glaciers in the Southern Sierra Nevada moved
415 faster than those in the central area. Our regional-scale InSAR study provides important baseline map of the kinematic states and useful guidance for field investigations and will be valuable for assessing the relationship of rock glaciers flow with regional climate and local conditions.

We also conduct a detailed InSAR study to map the surface flow of the Mount Gibbs rock glacier. We find two fast-moving branches in the lower part of the rock glacier, collocated with surface flow
420 lines. More interestingly, we observe a significant seasonal variability of surface speed, more than double in the fall from its minimum in the spring during the 2007–2008 season. Our findings suggest the necessity of a long time series with dense sampling to separate long-terms changes in rock glacier kinematics associated with climate change from seasonal variations.

Acknowledgements. We thank R.P. Daanen, O. Humlum, A. Kääh, T. Strozzi for their insightful reviews. B.
425 Collins (US Geological Survey, Menlo Park) and T. R. Lauknes (Norut) reviewed an early version of this paper. The ALOS PALSAR data are copyrighted by the Japan Aerospace Exploration Agency and provided by the Alaska Satellite Facility, University of Alaska Fairbanks. Climatic data at Lee Vining, CA are provided by the Western Regional Climate Center, NOAA. This research was supported primarily by the George Thompson Postdoctoral Fellowship to Lin Liu from the Department of Geophysics, Stanford University. Matlab and
430 Generic Mapping Tools (Wessel and Smith, 1998) were used to make the figures.

References

- Arenson, L., Hoelzle, M., and Springman, S.: Borehole deformation measurements and internal structure of some rock glaciers in Switzerland, *Permafrost Periglac.*, 13, 117–135, doi:10.1002/ppp.414, 2002.
- Avian, M., Kellerer-Pirklbauer, A., and Bauer, A.: LiDAR for monitoring mass movements in permafrost environments at the cirque Hinteres Langtal, Austria, between 2000 and 2008, *Nat. Hazards Earth Syst. Sci.*, 9, 1087–1094, doi:10.5194/nhess-9-1087-2009, 2009.
- 435
- Barsch, D.: Nature and importance of mass-wasting by rock glaciers in alpine permafrost environments, *Earth Surf. Processes*, 2, 231–245, doi:10.1002/esp.3290020213, 1977.
- Barsch, D.: *Rockglaciers: Indicators for the Present and Former Geocology in High Mountain Environments*, Springer, Berlin, 1996.
- 440
- Berardino, P., Fornaro, G., Lanari, R., and Sansosti, E.: A new algorithm for surface deformation monitoring based on small baseline differential SAR interferograms, *IEEE T. Geosci. Remote*, 40, 2375–2383, doi:10.1109/TGRS.2002.803792, 2002.
- Berger, J., Krainer, K., and Mostler, W.: Dynamics of an active rock glacier (Ötztal Alps, Austria), *Quaternary Res.*, 62, 233–242, doi:10.1016/j.yqres.2004.07.002, 2004.
- 445
- Berthling, I., Etzelmüller, B., Eiken, T., and Sollid, J. L.: Rock glaciers on Prins Karls Forland, Svalbard. I: internal structure, flow velocity and morphology, *Permafrost Periglac.*, 9, 135–145, doi:10.1002/(SICI)1099-1530(199804/06)9:2<135::AID-PPP284>3.0.CO;2-R, 1998.
- Bodin, X., Thibert, E., Fabre, D., Ribolini, A., Schoeneich, P., Francou, B., Reynaud, L., and Fort, M.: Two decades of responses (1986–2006) to climate by the Laurichard rock glacier, French Alps, *Permafrost Periglac.*, 20, 331–344, doi:10.1002/ppp.665, 2009.
- 450
- Brenning, A.: Geomorphological, hydrological and climatic significance of rock glaciers in the Andes of Central Chile (33–35° S), *Permafrost Periglac.*, 16, 231–240, doi:10.1002/ppp.528, 2005.
- Burger, K. C., Degenhardt Jr., J. J., and Giardino, J. R.: Engineering geomorphology of rock glaciers, *Geomorphology*, 31, 93–132, doi:10.1016/S0169-555X(99)00074-4, 1999.
- 455
- Chen, C. and Zebker, H.: Phase unwrapping for large SAR interferograms: statistical segmentation and generalized network models, *IEEE T. Geosci. Remote*, 40, 1709–1719, doi:10.1109/TGRS.2002.802453, 2002.
- Clark, D. H. and Gillespie, A. R.: Timing and significance of Late-glacial and Holocene cirque glaciation in the Sierra Nevada, California, *Quatern. Int.*, 38–39, 21–38, doi:10.1016/S1040-6182(96)00024-9, 1997.
- 460
- Clark, D. H., Clark, M. M., and Gillespie, A. R.: Debris-covered glaciers in the Sierra Nevada, California, and their implications for snowline reconstructions, *Quaternary Res.*, 41, 139–153, doi:10.1006/qres.1994.1016, 1994.
- Clow, D. W., Nanus, L., Verdin, K. L., and Schmidt, J.: Evaluation of SNODAS snow depth and snow water equivalent estimates for the Colorado Rocky Mountains, USA, *Hydrological Processes*, 26, 2583–2591, doi:10.1002/hyp.9385, <http://dx.doi.org/10.1002/hyp.9385>, 2012.
- 465
- Croce, F. A. and Milana, J. P.: Internal structure and behaviour of a rock glacier in the Arid Andes of Argentina, *Permafrost Periglac.*, 13, 289–299, doi:10.1002/ppp.431, 2002.
- Daly, C., Neilson, R. P., and Phillips, D. L.: A statistical-topographic model for mapping climatological precipitation over mountainous terrain, *J. Appl. Meteorol.*, 33, 140–158, doi:10.1175/1520-0450(1994)033<0140:ASTMFM>2.0.CO;2, 1994.
- 470

- Degenhardt Jr., J. J.: Development of tongue-shaped and multilobate rock glaciers in alpine environments – interpretations from ground penetrating radar surveys, *Geomorphology*, 109, 94–107, doi:10.1016/j.geomorph.2009.02.020, 2009.
- Delaloye, R., Perruchoud, E., Avian, M., Kaufmann, V., Bodin, X., Hausmann, H., Ikeda, A., Kääh, A., Kellerer-
475 Pirklbauer, A., Krainer, K., et al.: Recent Interannual variations of rockglaciers creep in the European Alps, in: Proceedings of the 9th International Conference on Permafrost, Fairbanks, Alaska, 2008.
- Delaloye, R., Lambiel, C., and Gärtner-Roer, I.: Overview of rock glacier kinematics research in the Swiss Alps: seasonal rhythm, interannual variations and trends over several decades, *Geogr. Helv.*, 65, 135–145, 2010.
- 480 Gesch, D., Oimoen, M., Greenlee, S., Nelson, C., Steuck, M., and Tyler, D.: The national elevation dataset, *Photogramm. Eng. Rem. S.*, 68, 5–11, 2002.
- Gruber, S. and Haerberli, W.: Permafrost in steep bedrock slopes and its temperature-related destabilization following climate change, *J. Geophys. Res.*, 112, F02S18, doi:10.1029/2006JF000547, 2007.
- Guneriusen, T., Hogda, K., Johnsen, H., and Lauknes, I.: InSAR for estimation of changes in snow water
485 equivalent of dry snow, *IEEE T. Geosci. Remote*, 39, 2101–2108, doi:10.1109/36.957273, 2001.
- Haerberli, W.: Creep of mountain permafrost: internal structure and flow of alpine rock glaciers, *Mit. Vers. Was.*, 77, 5–142, 1985.
- Haerberli, W., Kääh, A., Wagner, S., Mühl, D., Geissler, P., Haas, J., Glatzel-Mattheier, H., and Wagenbach, D.:
490 Pollen analysis and ¹⁴C age of moss remains in a permafrost core recovered from the active rock glacier Murtèl-Corvatsch, Swiss Alps: geomorphological and glaciological implications, *J. Glaciol.*, 45, 1–8, 1999.
- Harrison, S., Whalley, B., and Anderson, E.: Relict rock glaciers and protalus lobes in the British Isles: implications for Late Pleistocene mountain geomorphology and palaeoclimate, *J. Quaternary Sci.*, 23, 287–304, doi:10.1002/jqs.1148, 2008.
- Humlum, O.: The climatic significance of rock glaciers, *Permafrost Periglac.*, 9, 375–395,
495 doi:10.1002/(SICI)1099-1530(199810/12)9:4<375::AID-PPP301>3.0.CO;2-0, 1998.
- Humlum, O.: The geomorphic significance of rock glaciers: estimates of rock glacier debris volumes and head-wall recession rates in West Greenland, *Geomorphology*, 35, 41–67, doi:10.1016/S0169-555X(00)00022-2, 2000.
- Ikeda, A., Matsuoka, N., and Kääh, A.: Fast deformation of perennially frozen debris in a warm rock glacier in
500 the Swiss Alps: an effect of liquid water, *J. Geophys. Res.*, 113, F01021, doi:10.1029/2007JF000859, 2008.
- Isaksen, K., Ødegård, R. S., Eiken, T., and Sollid, J. L.: Composition, flow and development of two tongue-shaped rock glaciers in the permafrost of Svalbard, *Permafrost Periglac.*, 11, 241–257, doi:10.1002/1099-1530(200007/09)11:3<241::AID-PPP358>3.0.CO;2-A, 2000.
- Janke, J.: Long-term flow measurements (1961–2002) of the Arapaho, Taylor, and Fair rock glaciers, *Front Range, Colorado, Phys. Geogr.*, 26, 313–336, doi:10.2747/0272-3646.26.4.313, 2005.
- Johnson, B. G., Thackray, G. D., and Van Kirk, R.: The effect of topography, latitude, and lithology on rock glacier distribution in the Lemhi Range, central Idaho, USA, *Geomorphology*, 91, 38–50, doi:http://dx.doi.org/10.1016/j.geomorph.2007.01.023, http://www.sciencedirect.com/science/article/pii/S0169555X07000475, 2007.
- 510 Juliussen, H. and Humlum, O.: Thermal regime of openwork block fields on the mountains Elgåhogna and

- Sølen, central-eastern Norway, *Permafrost Periglac.*, 19, 1–18, doi:10.1002/ppp.607, 2008.
- Kääb, A.: Monitoring high-mountain terrain deformation from repeated air- and spaceborne optical data: examples using digital aerial imagery and ASTER data, *ISPRS J. Photogramm.*, 57, 39–52, doi:10.1016/S0924-2716(02)00114-4, 2002.
- 515 Kääb, A., Haeberli, W., and Gudmundsson, G. H.: Analysing the creep of mountain permafrost using high precision aerial photogrammetry: 25 years of monitoring Gruben rock glacier, Swiss Alps, *Permafrost Periglac.*, 8, 409–426, doi:10.1002/(SICI)1099-1530(199710/12)8:4<409::AID-PPP267>3.0.CO;2-C, 1997.
- Kääb, A., Frauenfelder, R., and Roer, I.: On the response of rockglacier creep to surface temperature increase, *Global Planet. Change*, 56, 172–187, doi:10.1016/j.gloplacha.2006.07.005, 2007.
- 520 Kenyi, L. and Kaufmann, V.: Estimation of rock glacier surface deformation using SAR interferometry data, *IEEE T. Geosci. Remote*, 41, 1512–1515, doi:10.1109/TGRS.2003.811996, 2003.
- Kistler, R. W.: Geologic map of the Mono Craters quadrangle, Mono and Tuolumne counties, California, Map GQ-462, Tech. rep., US Geological Survey, 1966.
- Konrad, S. K., Humphrey, N. F., Steig, E. J., Clark, D. H., Potter, N., and Pfeffer, W. T.: Rock glacier dynamics and paleoclimatic implications, *Geology*, 27, 1131–1134, 1999.
- 525 Krainer, K. and Mostler, W.: Reichenkar rock glacier: a glacier derived debris-ice system in the western Stubai Alps, Austria, *Permafrost Periglac.*, 11, 267–275, doi:10.1002/1099-1530(200007/09)11:3<267::AID-PPP350>3.0.CO;2-E, 2000.
- Lambiel, C. and Delaloye, R.: Contribution of real-time kinematic GPS in the study of creeping mountain permafrost: examples from the Western Swiss Alps, *Permafrost Periglac.*, 15, 229–241, doi:10.1002/ppp.496, 2004.
- 530 Leopold, M., Williams, M., Caine, N., Völkel, J., and Dethier, D.: Internal structure of the Green Lake 5 rock glacier, Colorado Front Range, USA, *Permafrost Periglac.*, 22, 107–119, doi:10.1002/ppp.706, 2011.
- Limpach, P., Geiger, A., Beutel, J., Buchli, B., Wirz, V., and Gruber, S.: Permanent monitoring of rock glaciers with low-cost GPS, in: 9th Swiss Geoscience Meeting, 273–273, 2011.
- 535 Lundquist, J. D. and Cayan, D. R.: Surface temperature patterns in complex terrain: daily variations and long-term change in the central Sierra Nevada, California, *J. Geophys. Res.*, 112, D11124, doi:10.1029/2006JD007561, 2007.
- Maurer, E.: Uncertainty in hydrologic impacts of climate change in the Sierra Nevada, California, under two emissions scenarios, *Climatic Change*, 82, 309–325, doi:10.1007/s10584-006-9180-9, 2007.
- 540 Millar, C. I. and Westfall, R. D.: Rock glaciers and related periglacial landforms in the Sierra Nevada, CA, USA; inventory, distribution and climatic relationships, *Quatern. Int.*, 188, 90–104, doi:10.1016/j.quaint.2007.06.004, available at: <http://nsidc.org/data/ggd652.html>, 2008.
- Millar, C. I., Westfall, R. D., and Delany, D. L.: Thermal and hydrologic attributes of rock glaciers and periglacial talus landforms, Sierra Nevada, California, USA, *Quatern. Int.*, doi:10.1016/j.quaint.2012.07.019, in press, 2012.
- 545 Nagler, T., Mayer, C., and Rott, H.: Feasibility of DINSAR for mapping complex motion fields of alpine ice- and rock-glaciers, in: *Retrieval of Bio- and Geo-Physical Parameters from SAR Data for Land Applications*, edited by: Wilson, A. and Quegan, S., Vol. 475 of ESA Special Publication, 377–382, 2002.
- 550 Nötzli, J. and Vonder Muehll, D. (Eds.): *Permafrost in Switzerland 2006/2007 and 2007/2008*, Glaciological

- Report (Permafrost), The Cryospheric Commission of the Swiss Academy of Sciences, 2010.
- Perruchoud, E. and Delaloye, R.: Short-term changes in surface velocities on the Becs-de-Bosson rock glacier (western Swiss Alps), in: Proceedings of the 9th International Symposium on High Mountain Remote Sensing Cartography (HMRSC-IX), vol. 43, 14–15, 2007.
- 555 Potter, N. J., Steig, E. J., Clark, D. H., Speece, M. A., Clark, G. M., and Updike, A. B.: Galena Creek rock glacier revisited: new observations on an old controversy, *Geogr. Ann. A*, 80, 251–265, 1998.
- Rignot, E., Hallet, B., and Fountain, A.: Rock glacier surface motion in Beacon Valley, Antarctica, from synthetic-aperture radar interferometry, *Geophys. Res. Lett.*, 29, 1607, doi:10.1029/2001GL013494, 2002.
- Roer, I., Kääb, A., and Dikau, R.: Rockglacier kinematics derived from small-scale aerial photography and
560 digital airborne pushbroom imagery, *Zeitschrift für Geomorphologie N.F.*, 49, 73–87, 2005.
- Rott, H. and Siegel, A.: Analysis of mass movements in alpine terrain by means of SAR interferometry, in: Geoscience and Remote Sensing Symposium, 1999, IGARSS '99 Proceedings, IEEE 1999 International, vol. 4, 1933–1936, doi:10.1109/IGARSS.1999.774991, 1999.
- Serreze, M. C., Clark, M. P., Armstrong, R. L., McGinnis, D. A., and Pulwarty, R. S.: Characteristics of the
565 western United States snowpack from snowpack telemetry (SNOTEL) data, *Water Resources Research*, 35, 2145–2160, doi:10.1029/1999WR900090, <http://dx.doi.org/10.1029/1999WR900090>, 1999.
- Strozzi, T., Kääb, A., and Frauenfelder, R.: Detecting and quantifying mountain permafrost creep from in situ inventory, space-borne radar interferometry and airborne digital photogrammetry, *Int. J. Remote Sens.*, 25, 2919–2931, doi:10.1080/0143116042000192330, 2004.
- 570 Wagner, S.: Creep of alpine permafrost, investigated on the murtel rock glacier, *Permafrost Periglac.*, 3, 157–162, doi:10.1002/ppp.3430030214, 1992.
- Wahrhaftig, C. and Cox, A.: Rock glaciers in the Alaska range, *Geol. Soc. Am. Bull.*, 70, 383–436, 1959.
- Wessel, P. and Smith, W. H. F.: New, improved version of generic mapping tools released, *EOS T. Am. Geophys. Un.*, 79, 579–579, doi:10.1029/98EO00426, 1998.
- 575 Whalley, W. B. and Martin, H. E.: Rock glaciers: II Models and mechanisms, *Prog. Phys. Geogr.*, 16, 127–186, 1992.
- Zebker, H. A. and Villasenor, J.: Decorrelation in interferometric radar echoes, *IEEE T. Geosci. Remote*, 30, 950–959, 1992.
- Zebker, H., Hensley, S., Shanker, P., and Wortham, C.: Geodetically Accurate InSAR Data Processor, *IEEE T. Geosci. Remote*, 48, 4309–4321, doi:10.1109/TGRS.2010.2051333, 2010.
580

Table 1. Interferograms made from the case study on the Mount Gibbs rock glacier. Names of interferograms are in the format “yyyymmdd–yyyymmdd”, after the dates of the two SAR scenes used. Column “B perp” lists the perpendicular baselines of the interferograms.

Interferogram	Timespan (days)	B perp (m)	Path/Frame
20070402–20070518	46	–286	216/750
20070402–20070703	92	92	216/750
20070402–20070818	138	315	216/750
20070518–20070703	46	378	216/750
20070518–20070818	92	601	216/750
20070703–20070818	46	223	216/750
20070904–20071205	92	349	217/740
20071003–20080103	92	354	216/750
20071020–20071205	46	109	217/740
20071020–20080120	92	534	217/740
20071205–20080120	46	424	217/740
20080103–20080520	92	1218	216/750

Table 2. Summary of the active rock glaciers in the Sierra Nevada based on InSAR and comparisons with the “active” cirque rock glaciers in the Millar and Westfall (2008) (MW) database. The term “active” used by the MW database is based on the geomorphological and hydrological features (see Sect. 4.1).

	InSAR	MW
Number	59	67
Mean elevation (m)	3551	3390
Elevation range (m)	3077–3787	2673–3901
Mean size (ha)	13	20
Size range (ha)	3–46	N/A
Mean length (m)	624	N/A
Mean width (m)	201	N/A
Mean length-to-width ratio	3.3	N/A
Mean flow speed (cm yr ⁻¹)	53	N/A
Flow speed range (cm yr ⁻¹)	14–87	N/A

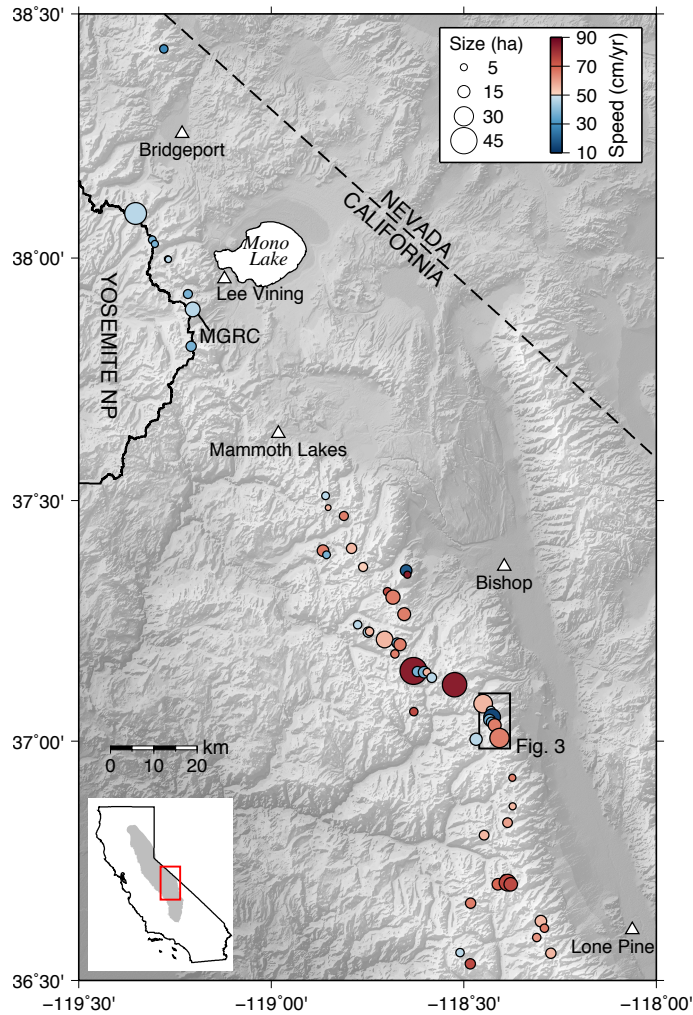


Fig. 1. Map of the study area in the central Sierra Nevada of California, USA. Circles are active rock glaciers based on our InSAR measurements. The size and color of the circles represent the size and speed of the rock glaciers, respectively. “MGRC” stands for the Mount Gibbs Rock Glacier. The black box outlines the area shown in Fig. 3. The inset map of California shows the Sierra Nevada in gray and the location of the study area as a red box.

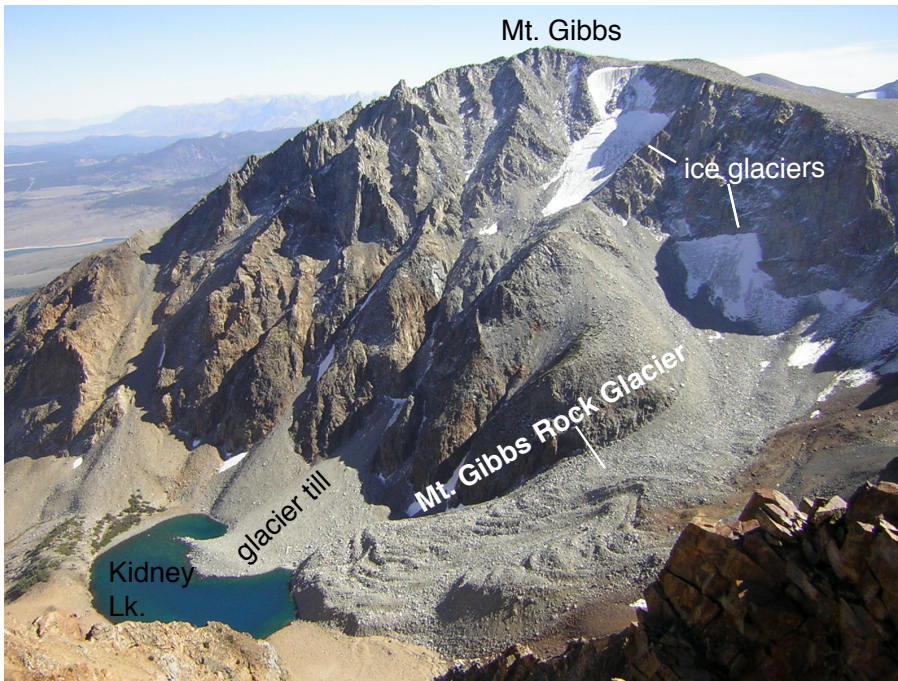


Fig. 2. The Mount Gibbs rock glacier from the shoulder of Mount Dana looking south (Photo: C. Millar).

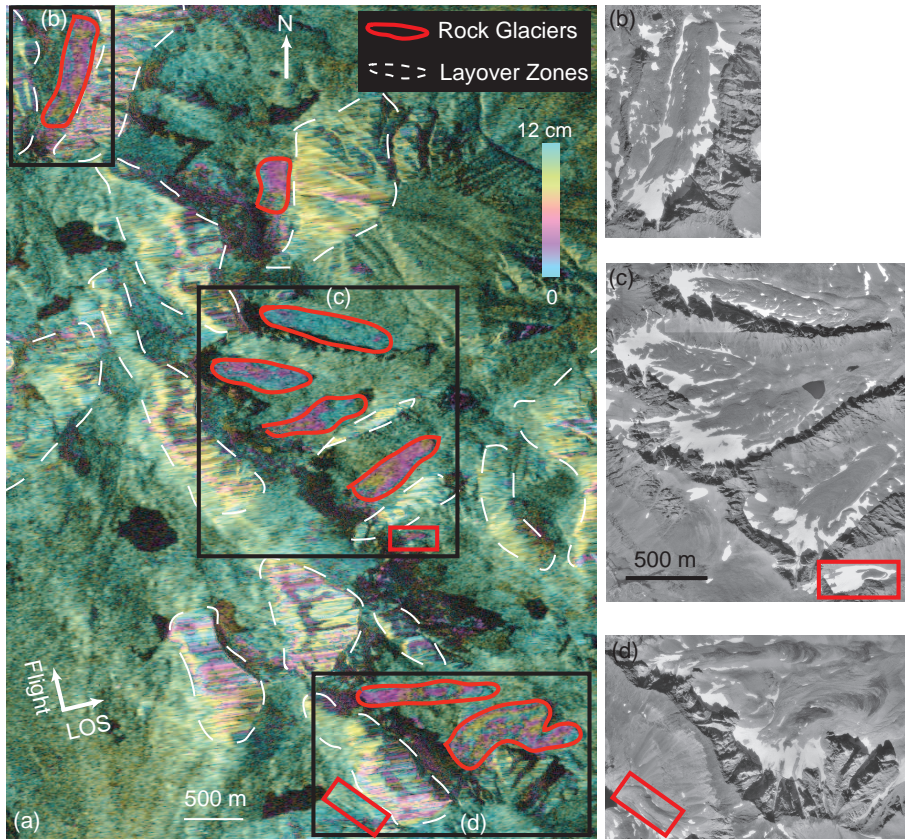


Fig. 3. (a) Wrapped and geocoded PALSAR interferogram spanning 18 August 2007 to 3 October 2007 (Path 216, Frame 730). Background is the radar intensity image. Actively-moving areas of rock glaciers are outlined by red polygons. Red boxes outline two rock glaciers not included in our inventory (see Sect. 3.2). White dashed polygons outline radar layover zones. Satellite flight and line-of-sight (LOS) directions are plotted as perpendicular vectors. (b–d) are aerial photos of the areas defined in (a). These photos were taken in late summer of 1998 and produced by the USDA Geospatial Service and Technology Center. All photos are to the same scale shown in (c).

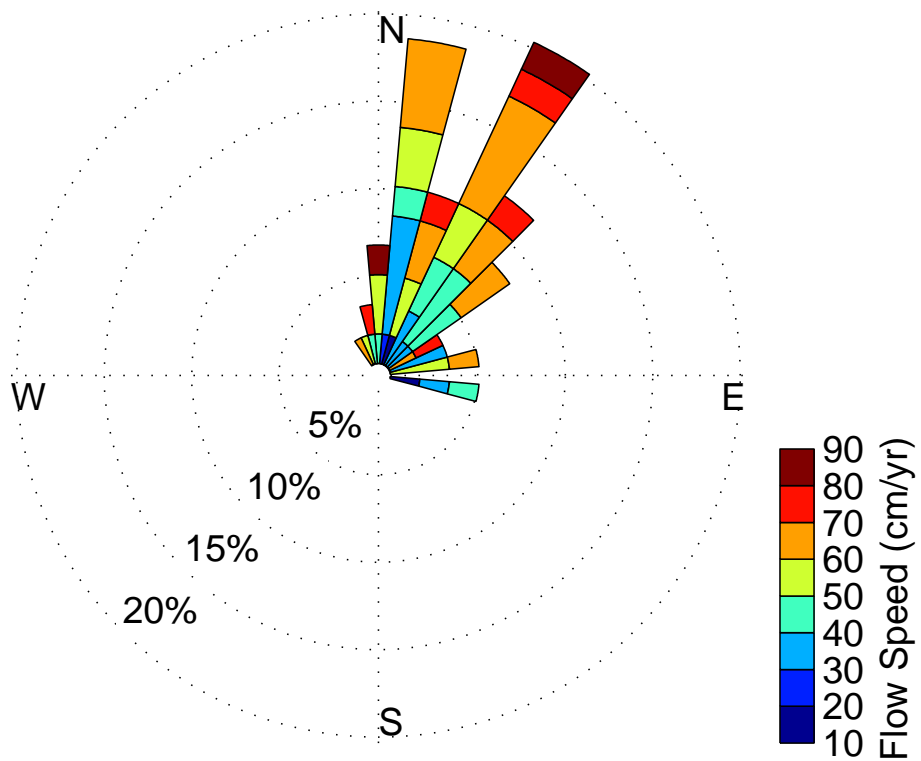


Fig. 4. Histogram of rock glacier flow aspects and speeds, plotted as a wind rose diagram. The radius of each triangle represents the frequency of the rock glacier aspects within each bin (10 degrees wide). Each triangle is subdivided into color-coded bands that show flow speed ranges.

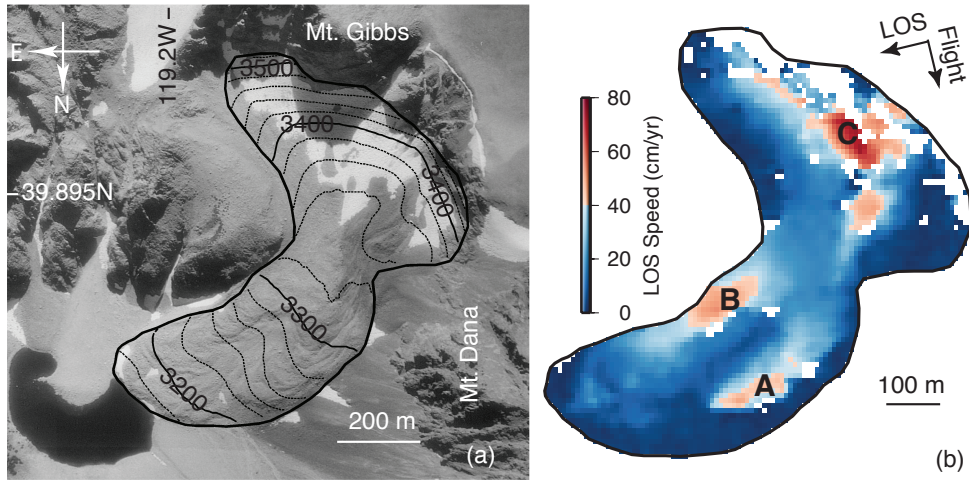


Fig. 5. (a) Aerial photo of the Mount Gibbs rock glacier, taken on 25 September 1993. Rock glacier boundary is roughly outlined by the solid black line. Dashed lines are topographic contours spaced at 20 m. (b) InSAR line-of-sight speed during 4 September 2007 and 5 December 2007. White areas within the black boundary are places of low interferometric coherence. “A”, “B”, and “C” mark the center of fast-moving areas. Both (a) and (b) are rotated clockwise by 180 degrees to match the viewing geometry of Fig. 2. North and east directions are denoted in (a).

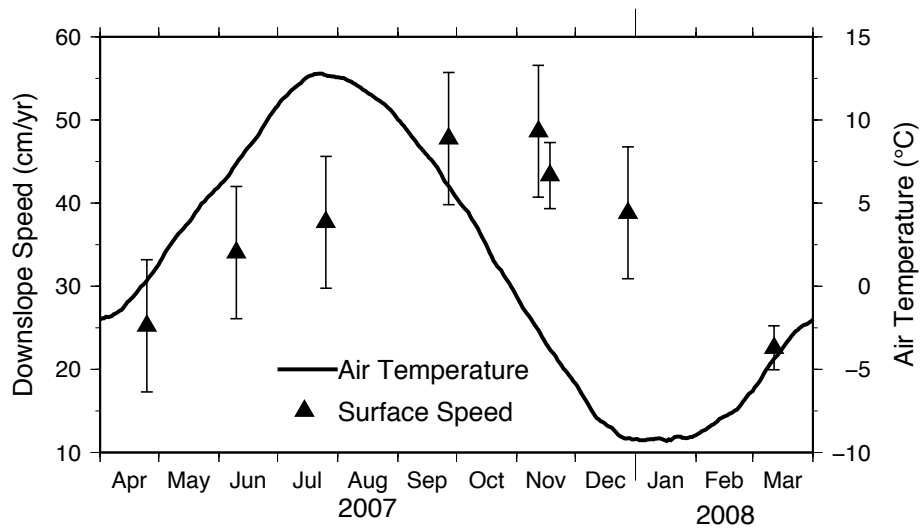


Fig. 6. Time series of the estimated air temperature (solid line) and the InSAR-measured downslope speed (triangles) at the marker “A” shown in Fig. 5b. The error bars are the 1- σ uncertainties of the measured speed.